Changes in Arctic vegetation amplify high-latitude warming through the greenhouse effect

Abigail L. Swann[a,1], Inez Y. Fung[a], Samuel Levis[b], Gordon B. Bonan[b], and Scott C. Doney[c]

[a]Department of Earth & Planetary Science, University of California, Berkeley, CA 94720; [b]National Center for Atmospheric Research, Boulder, CO 80307; and [c]Department of Marine Chemistry and Geochemistry, Woods Hole Oceanographic Institution, Woods Hole, MA 02543

Contributed by Inez Y. Fung, December 4, 2009 (sent for review October 20, 2009)

Arctic climate is projected to change dramatically in the next 100 years and increases in temperature will likely lead to changes in the distribution and makeup of the Arctic biosphere. A largely deciduous ecosystem has been suggested as a possible landscape for future Arctic vegetation and is seen in paleo-records of warm times in the past. Here we use a global climate model with an interactive terrestrial biosphere to investigate the effects of adding deciduous trees on bare ground at high northern latitudes. We find that the top-of-atmosphere radiative imbalance from enhanced transpiration (associated with the expanded forest cover) is up to 1.5 times larger than the forcing due to albedo change from the forest. Furthermore, the greenhouse warming by additional water vapor melts sea-ice and triggers a positive feedback through changes in ocean albedo and evaporation. Land surface albedo change is considered to be the dominant mechanism by which trees directly modify climate at high-latitudes, but our findings suggest an additional mechanism through transpiration of water vapor and feedbacks from the ocean and sea-ice.

biosphere-atmosphere interaction | climate feedback | radiative forcing | sea-ice | deciduous

The range of high-latitude trees is expected to expand poleward with warming and, in fact, the northern tree line is moving northward now (1). Changes in vegetation cover are recognized to modify climate and the energy budget of the earth through changes in albedo in high latitudes and evapo-transpiration (ET) in the tropics (2, 3). In snow-covered regions, the springtime growth of leaves enhances solar absorption because surface albedo is reduced from that of snow (~0.8) towards that of leaves (~0.1). Leaves also play a hydrologic role, transpiring water from the soil to the atmosphere. Variations in albedo and transpiration rates between different types of vegetation will induce a climate response that may depend on vegetation type. It has been suggested that broad-leaf deciduous trees may invade warming tundra more effectively than boreal evergreen trees (4) and, due to the higher rates of transpiration and a higher albedo of deciduous broad-leaf trees compared to needle-leaf evergreen trees (5), we expect that the climate response may be different.

Previous studies on the climatic effects of changes in the distribution of Arctic vegetation have focused primarily on the range expansion or contraction of evergreen needle-leaf trees (6–10). The dark color and low ET of evergreen needle-leaf trees leads to a dramatic change in albedo, and thus short-wave forcing, with the addition or removal of trees but little change in long-wave forcing (e.g. ref. 6, ref. 7). Deciduous broad-leaf trees in the Arctic have twice the albedo and 50–80% greater ET rates when leafed-out than their evergreen needle-leaf counterparts (11). It has been suggested that a vegetation change from evergreen to deciduous (such as after a disturbance) will produce a surface cooling due to the increase in albedo and latent cooling (e.g. ref. 11, ref. 5). Eugster et al. (ref. 12) acknowledge that ecosystem changes that increase ET could also increase atmospheric moisture content but they consider this important only as a consequence for cloudiness (with increased moisture leading to an increase in cloud cover) and leave the total effect on the energy budget unresolved. McGuire et al. (ref. 13) assume that changes in atmospheric water vapor due to imports from lower latitudes to be important for the climate of the Arctic but do not directly consider changes in atmospheric moisture related to changes in vegetation. In fact, they explicitly state that the only three ways in which climate is coupled to vegetation in the Arctic are albedo, energy partitioning at the surface, and the emission of greenhouse gases.

If tree expansion with climate warming occurs by deciduous broad-leaf trees as is suggested by some studies of future warming (14) and observations of past vegetation (4, 15) we might expect both short-wave and long-wave effects to be significant. The vegetation change we consider here is not the shift within the boreal forest from evergreen to deciduous, but an expansion of deciduous forest into previously unvegetated areas.

It is difficult to determine the timing of species invasion either from observations or modeling. Qualitative statements based on observations are made about "rapid" changes (e.g., ref. 4, ref. 16), and model estimates have been made for the rate of vegetation changes under future climate scenarios (e.g. ref. 17, ref. 14), but we have been unable to find an estimate of the potential rate of expansion of deciduous forest as we are considering in our manuscript. Based on observations and modeling work that has been done we suggest that it is not unreasonable to assume that the expansion of deciduous trees could happen regionally on time scales shorter than the time for the climate to reach a new equilibrium in 10^3 years.

This study is intended to identify which processes must be considered when evaluating the effects of vegetation changes on climate in the Arctic. We aim to constrain the relative effects of changes in short-wave (albedo) and long-wave (atmospheric water vapor from ET) forcing as a result of the expansion of deciduous broad-leaf trees at high-northern latitudes.

Results

Climate Response to Expansion of Deciduous Forest. We performed four equilibrium simulations using a coupled atmosphere-land-carbon cycle global model, using two representations of vegetation cover (present day land cover and expanded vegetation with deciduous trees on bare ground north of 60 °N (Fig. 1)) and two ocean representations (interactive ocean (IO) and fixed ocean (FO)—see *Methods* section). Anomalies, represented by $\Delta\phi$, are reported as the difference in climate variable ϕ simulated by the experiments with expanded forest cover and present day vegetation distribution with the same ocean module (either ΔV – IO or ΔV-FO). The vegetation interacts with climate through changing stomatal conductance, leaf area, and mass and hence albedo and transpiration. The ΔV-FO anomalies are an approximation of the response to direct forcing from vegetation expansion as any feedbacks associated with changes in ocean

Author contributions: A.L.S., I.Y.F., S.L., G.B.B., and S.C.D. designed research and wrote the paper; A.L.S. and S.L. performed research; and A.L.S. analyzed data.

The authors declare no conflict of interest.

Freely available online through the PNAS open access option.

[1]To whom correspondence should be addressed at: E-mail: aswann@atmos.berkeley.edu.

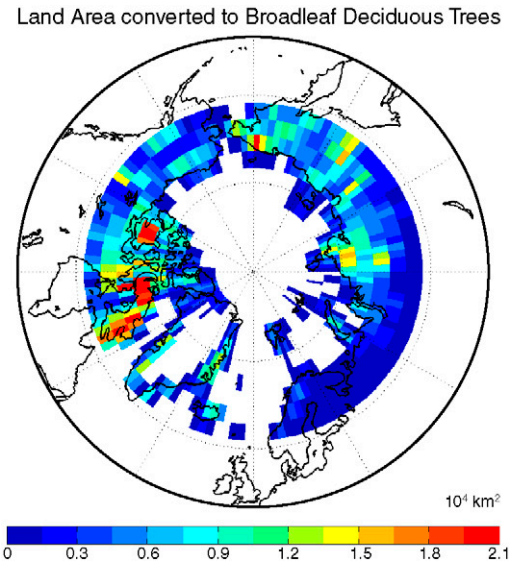

Fig. 1. Map showing the land area converted to broad-leaf deciduous trees in V-FO and V-IO in units of 10^4 km^2. The converted area totals 3, 000, 000 km^2.

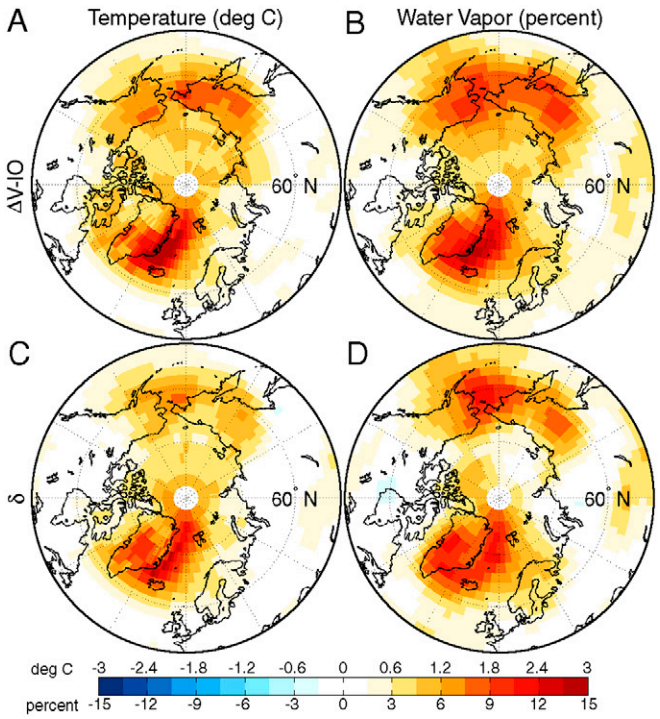

Fig. 2. (*A*) The anomaly (ΔV – IO) in near-surface atmospheric temperature in degrees Celcius (deg C) between a model experiment where trees are introduced on bare ground north of 60 °N and a corresponding control run with no added trees. (*B*) The same as (*A*) for column water vapor in percent. (*C*) The difference δ(ΔV – IO-ΔV-FO) in near-surface atmospheric temperature in deg C between two anomalies where trees are introduced on bare ground north of 60 °N, one with an interactive ocean model (V-IO), and the other with fixed ocean and sea-ice (V-FO). (*D*) The same as (*C*) for column water vapor in percent.

temperature or sea-ice-cover are damped. The ΔV – IO anomalies can be considered as the whole earth system response including the response both to direct forcing and any associated feedbacks. The difference between the two anomalies, $\delta\Delta\phi = \Delta\phi(\Delta V - IO) - \Delta\phi(\Delta V - FO)$, represents the additional feedback (from both land and ocean) experienced when the ocean and sea-ice are allowed to adjust.

The expansion of trees at high-northern latitudes leads to an annual mean near-surface atmosphere warming (ΔT) of 1 and 0.2 K over the Arctic (all area north of 60 °N) for ΔV – IO and ΔV-FO, respectively. The spatial pattern of ΔT is widespread in both the annual mean (Fig. 2*A* and *C*) and throughout the year (Table 1). The phasing of peak ΔT is shifted to spring (in both FO and IO) in contrast to winter polar amplification associated with greenhouse gas forcing (18). The annual mean ΔT comes about as a result of land and ocean feedbacks to the initial forcing from northern expansion of Arctic vegetation but does not have an identical spatial pattern (Fig. 1, Fig. 2*A*).

Feedbacks over both land and ocean (in IO runs) amplify the warming forced directly by changes in vegetation. Over the ocean, warming leads to a reduction in sea-ice area (13% in July, 26% in September) which, in turn, decreases ocean albedo by 8% (blue dashed line with "+" Fig. 3*A*) and increases the evaporative flux by 21% in July (blue dashed line with "+" Fig. 3*B*). Sea surface temperatures and ice area are held constant in the V-FO case, but Δalbedo over the ocean is nonzero as snow and cloud cover are allowed to change (blue dashed line with "o" Fig. 3*A*).

Low cloud cover anomalies are negative over both land and ocean (by up to 8% in ΔV – IO), but the change is not significant. The decrease in low cloud is due to an increase in stability from warming aloft. This is counter to the assertion of Eugster et al. (ref. 12) who state (but do not test) that increases in ET from adding deciduous vegetation should increase cloudiness.

The expansion of trees in the Arctic has two direct implications for climate. First, there is a decrease in surface albedo over land in the springtime (green solid line in Fig. 3*A*) as relatively dark stems and leaves cover bright snow. Leaf-out occurs across the Arctic in June, but stem area and a small residual leaf area are maintained throughout the year and mask snow area causing the largest albedo change when the sun comes out in April and May. Second, there is enhanced ET in the summer (red dashed dot line in Fig. 3*B*) leading to an increase in atmospheric water vapor and consequently the greenhouse effect. The increase in ET also cools at the surface, but the latent cooling is too small to overcome the greenhouse warming from the increase in water vapor and direct heating from the increase in absorbed solar radiation leading to a net warming. Almost all ΔET over land comes from transpiration (compare green solid line and red dashed dot line in Fig. 2*B*) but with the increase in ET there is a slight compensating decrease in soil evaporation.

The addition of trees causes both a decrease in albedo and an increase in water flux from transpiration. Warmer air holds more water vapor than colder air thus we expect water vapor in the atmosphere will increase, somehow, in response to increases in temperature. It is very difficult, if not impossible, to isolate the initial effect of the water vapor directly released from enhanced transpiration (the "trigger") from the water vapor resulting from a subsequent increase in temperature (the "response"), as the distribution of both ΔT and δΔT covaries with column water vapor increase (Fig. 2).

Precipitation minus evaporation ($P - E$) is generally positive in the Arctic, i.e. there is a net import of water vapor from lower latitudes. The effective water vapor import anomalies, calculated by closing the water budget (see *Methods* section), shows a decrease in net import from lower latitudes in July for ΔV – IO and April ΔV-FO. The July reduction in import of water occurs when ΔT is the largest and corresponds with the summer growing season confirming that the increase in column water vapor comes from within Arctic inputs of water to the atmosphere.

Direct Comparison of Forcing Mechanisms. To explicitly separate the effects of albedo and changes in water vapor on the net radiative imbalance (ΔF) at the top of the atmosphere, we performed a

Table 1. Change in Climate model variables with the northward expansion of trees

			Fixed Ocean						Interactive Ocean					
			Land			Ocean			Land			Ocean		
Month	Variable Name	Units	C-FO	ΔV-FO	p	C-FO	ΔV-FO	p	C-IO	ΔV – IO	p	C-IO	ΔV – IO	p
April														
	Surf. Air Temp.	K	265.04	**0.98**	**0.0070**	260.76	0.28	0.5043	265.56	**1.48**	**0.0038**	261.46	**1.46**	**0.0044**
	Water Vapor	Kgm^{-2}	6.09	0.03	0.9000	5.54	0.20	0.2890	6.21	0.32	0.1633	5.69	**0.39**	**0.0438**
	Low Cloud	fraction	0.58	-0.03	0.4483	0.63	-0.02	0.6728	0.58	-0.05	0.3287	0.64	-0.02	0.5771
	Albedo	albedo	0.51	**-0.07**	**0.0013**	0.60	-0.004	0.7917	0.50	-0.08	0.2556	0.59	-0.01	0.8429
	Latent Heat	Wm^{-2}	10.07	**1.39**	**0.0305**	17.00	**-2.59**	**0.0000**	10.19	**1.52**	**0.0202**	16.28	0.65	0.1430
	Sensible Heat	Wm^{-2}	12.15	1.30	0.0570	15.08	**-3.29**	**0.0000**	11.75	0.81	0.2229	14.60	**-1.86**	**0.0033**
	Ice Fraction	fraction	na	na	na	0.70	0.00	1.0000	na	na	na	0.70	-0.01	0.8755
	Precipitation	$10^{-8}\,m\ s^{-1}$	1.37	-0.03	1.0000	1.08	0.03	1.0000	1.38	-0.03	1.0000	1.16	0.00	1.0000
	Eff. Water Import	kgs^{-1}	na	na	na	304.37	**-20.25**	**0.0000**	na	na	na	300.69	0.09	0.9736
	Transpiration	Wm^{-2}	0.95	0.16	0.4582	na	na	na	1.12	0.20	0.4184	na	na	na
July														
	Surf. Air Temp.	K	284.88	0.51	0.2236	277.49	0.09	0.8375	284.98	**1.09**	**0.0455**	277.63	0.82	0.1794
	Water Vapor	Kgm^{-2}	19.35	0.38	0.1316	17.21	0.20	0.2850	19.38	**0.89**	**0.0047**	17.53	**0.50**	**0.0289**
	Low Cloud	fraction	0.49	-0.02	0.5910	0.75	-0.01	0.7834	0.48	-0.02	0.6227	0.75	-0.02	0.7138
	Albedo	albedo	0.24	-0.01	0.4898	0.23	0.00	0.9501	0.24	-0.01	0.8149	0.23	-0.02	0.6458
	Latent Heat	Wm^{-2}	43.34	**4.16**	**0.0000**	12.49	**-1.10**	**0.0051**	44.20	**5.29**	**0.0000**	12.92	**2.66**	**0.0000**
	Sensible Heat	Wm^{-2}	19.98	1.00	0.2169	4.34	-0.23	0.6746	20.13	0.52	0.4956	4.17	1.19	0.0558
	Ice Fraction	fraction	na	na	na	0.36	0.00	1.0000	na	na	na	0.36	-0.05	0.4100
	Precipitation	$10^{-8}\,m\ s^{-1}$	2.53	0.03	1.0000	1.17	-0.05	1.0000	2.46	0.13	0.9999	1.22	-0.01	1.0000
	Eff. Water Import	kgs^{-1}	na	na	na	321.72	1.07	0.6725	na	na	na	313.68	**-8.38**	**0.0030**
	Transpiration	Wm^{-2}	17.16	**4.61**	**0.0000**	na	na	na	17.65	**5.55**	**0.0000**	na	na	na

Variables of interest are shown from the four global climate model runs. Values are reported as the mean of the control run (C-FO and C-IO), the anomaly (ΔV-FO or ΔV – IO), and *p*-value of significance for spatial averages over either land (1.3×10^8 km^2) or ocean (3.4×10^8 km^2) area north of 60 °N. *P*-values of 0.05 or less indicate significance of at least 95% confidence and are shown in bold. The exception is effective water import (see *Methods*) which is an estimate of the monthly average of atmospheric water vapor imported northward over the 60 °N latitude line.

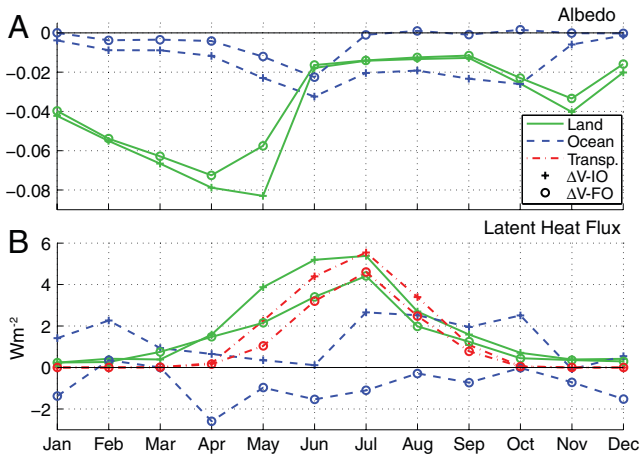

Fig. 3. (*A*) Albedo anomalies averaged over land area north of 60 °N (*Green* solid line), ocean area north of 60 °N (*Blue* dashed line). Plus signs represent results from the interactive ocean model (ΔV – IO) and open circles represent results from the fixed ocean model (ΔV-FO). (*B*) Same as for (*A*) for latent heat flux anomalies and transpiration averaged over land area north of 60 °N (*Red* dashed-dot line).

sensitivity analysis using a one-dimensional offline version of the radiation calculations from our atmospheric model (see *Methods* section). As with the full global model experiments, the FO conditions are used to estimate the "direct" effect of adding trees (as the response of the system is damped by the fixed ocean) and the $\delta\Delta F$ ($\Delta V - IO$ minus ΔV-FO) is used to estimate feedbacks. Adding trees to the bare ground in the Arctic causes a "direct" increase in ΔF over land of 0.96 Wm^{-2} due to the decrease in albedo and of 0.95 Wm^{-2} due to increased water vapor from transpiration (shaded area of first two columns in Fig. 4). The net radiative imbalance is amplified when the ocean is allowed to respond ($\delta\Delta F$, nonshaded area in columns in Fig. 4) due to an increase in terrestrial productivity and a consequent (*i*) darkening of the land surface by additional leaves (0.23 Wm^{-2}), (*ii*) additional increase in water vapor from ET (0.44 Wm^{-2}), and (*iii*) "indirect" feedbacks from the increase in sea surface temperature and melting of sea-ice (0.44 Wm^{-2} from ocean albedo and 0.94 Wm^{-2} from evaporation changes). With the full response of both atmosphere and ocean, the ΔF over land due to anomalous water vapor from ET is substantial and of the same magnitude as the direct ΔF due to albedo change.

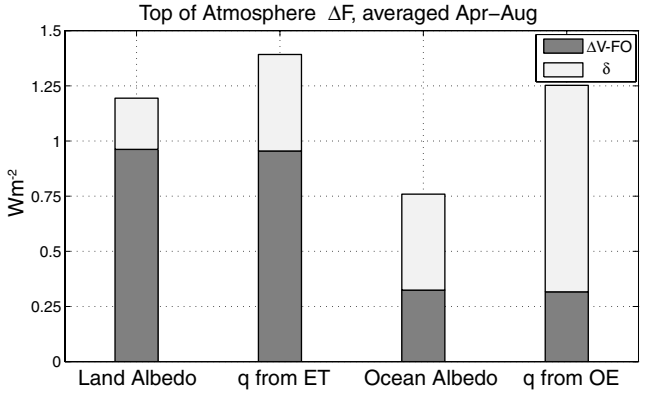

Fig. 4. The top-of-atmosphere net radiative imbalance (ΔF) caused by adding trees. Terms shown (from *Left* to *Right*) are ΔF due to changes in land albedo, water vapor changes from evapo-transpiration (ET), ocean albedo, water vapor changes from ocean evaporation (OE). The total value of each column shows the full ΔF from $\Delta V - IO$. The dark color shows the direct response of ΔV-FO and the light color shows the additional feedback $\delta(\Delta V - IO\text{-}\Delta V\text{-FO})$ when the ocean and sea-ice are allowed to respond.

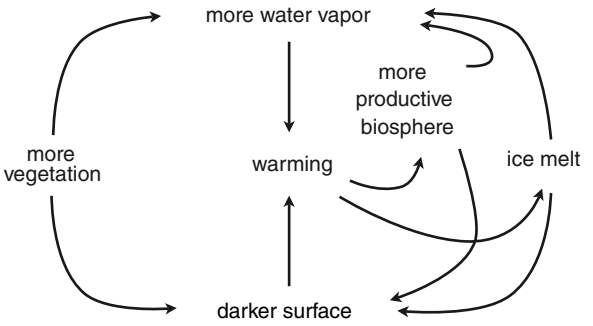

Fig. 5. Diagram representing the response and feedback of vegetation and sea-ice processes on climate at high-northern latitudes.

Our hypothesis is as follows (Fig. 5): Expansion of deciduous forest causes a darkening of the surface due to the masking of bright snow by relatively dark stems and leaves and a concomitant increase in transpiration by the new leaves. These initial forcings, the lowering of albedo, and increase in column water vapor, cause an increase in surface temperature over land. Water transpired by plants is efficiently mixed throughout the Arctic leading to surface warming over the ocean. Warming over the ocean, in turn, leads to the melting of sea-ice (in $\Delta V - IO$) resulting in a darker ocean surface as well as an increase in evaporation from the warmer ocean and newly ice-free water. This feedback chain warms the land surface further leading to greater productivity, lower albedo, and greater transpiration. The total temperature change seen in $\Delta V - IO$ includes both the initial forcing and all consecutive feedbacks listed here.

Discussion and Summary

We find that expansion of deciduous trees in the Arctic modifies both the short-wave and long-wave energy budgets, and initiates additional positive feedbacks associated with decreased sea-ice albedo and enhanced water vapor from evaporation from the Arctic Ocean. In particular, our analysis of the radiative energy imbalance due to the radiative forcing effects of water vapor is of the same order of magnitude as short-wave forcing from albedo changes. Thus, this study does not support the conventional wisdom (e.g. ref. 3, ref. 11) that land albedo is the dominant means by which terrestrial vegetation interacts with climate at high-northern latitudes.

The temperature increase obtained in this experiment (~1 degree across the Arctic) is modest in the global context but suggests that changing land cover in the Arctic could amplify an ongoing warming. The total ΔF over land due to water vapor from increased transpiration alone (1.4 Wm^{-2}), while regional, falls in between the estimated regional forcing (north of 60 °N) from CO_2 of an increase from 291 ppm to 370 ppm (1.1 $W\,m^{-2}$) and from 291 ppm to 437 ppm (1.85 Wm^{-2}) (19).

The expansion of deciduous woodlands has been observed in past times of warming (4, 15), and is predicted by some studies of future warming (14). Our study shows that the expansion of deciduous forest has a positive feedback on regional climate change. We suggest that an increase in deciduous woodland coverage might accelerate further expansion as warming provides more favorable growing conditions for deciduous trees at high-northern latitudes. We find a number of aspects of hydrology counter to stated (but untested) assumptions about the climatic role of deciduous vegetation from ecological literature (e.g. an expected increase in cloud cover (12) or the role of ET (5, 11)). This study does not investigate the timescale associated with expansion and therefore we cannot say if this is a mechanism that might lead to abrupt change. However, it suggests that vegetation changes create a positive feedback through albedo and transpiration and produce a strong warming if they act in combination with

sea-ice processes. The long-wave effects from changes in atmospheric moisture are not generally considered in studies of high-latitude vegetation change, but we find the radiative forcing from water vapor to be the same magnitude as the direct short-wave forcing from albedo, indicating that the energy budget of the entire column should be considered and not just the balance of surface fluxes.

Methods

Climate Response to Expansion of Deciduous Forest. To investigate the role of vegetation changes at high-latitudes, we use the National Center for Atmospheric Research Community Atmosphere and Land models with an interactive carbon cycle (CAM 3.0-CLM 3.5-CASA′) (20–22). Bare ground (nonglacier, nonlake, nonvegetated land) north of 60 °N is converted to broad-leaf deciduous trees and all previously designated vegetation is left unmodified, as are glaciers and lakes. The converted area totals 3, 000, 000 km^2 (1.75 times the size of Alaska). The primary regions converted to deciduous forest vegetation are the Canadian Archipelago, the Taymyr Peninsula, and Chukotka in Russia (Fig. 1). This particular conversion (from bare ground to forest) is used to make the simplest comparison possible by looking only at one vegetation transition. The exact distribution of vegetation used in these simulations may not reflect the regional patterns expected with warming, but the analysis is primarily focused on identifying the processes which control vegetation-climate interactions at these latitudes and not on the regional pattern of response.

The model control (C, standard land cover) and experiment (V, modified land cover) are each run with two representations of the ocean: An interactive slab ocean model (IO) with thermodynamic sea-ice (23), and a fixed ocean (FO) wherein sea surface temperature and sea-ice are set to the monthly mean conditions in the C-IO control run. The four model runs are integrated for 30 yr, and the results presented are averages of the last 20 yr. The simulation length of 20 yr is sufficient to bring climate variables into equilibrium. Values in Table 1 are reported as the mean for one month (April and July) over either the land or ocean area north of 60 °N except for water import, which is reported as the flux across the 60 °N latitude line. Significance is calculated using an estimated 10 degrees of freedom for each 20-year period and reported as p-values where a p-value of 0.05 indicates that we reject the null hypothesis that the anomaly is zero with 95% confidence (shown in bold).

Water Budget of the Arctic. The Arctic north of 60 °N can be considered an isolated system in the model in which all terms in the water budget can be explicitly identified. Inputs to atmospheric water vapor in the Arctic include fluxes from the land surface (transpiration, canopy evaporation, ground evaporation) fluxes from the ocean (evaporation) and imports of water via advection across the 60 °N latitude line. The only export from the atmosphere is precipitation.

Due to the mass fixer in the nonconservative semilagrangian transport scheme, we cannot calculate the actual model transport of water vapor (24). We are able to estimate model transport, but using this estimate we cannot close the water budget, even on annual time scales, indicating that the estimated transport is far from the actual transport experienced in the model. As the true model transport is unknown and the turnover time of water in the Arctic is assumed to be of order 10 d, we infer an effective transport for each month as the residual of $P - E$ (including transpiration, canopy evaporation, ground evaporation, and ocean evaporation). This effective import is used in Table 1.

Direct Comparison of Forcing Mechanisms. We calculate top-of-atmosphere energy imbalance (ΔF) for each forcing term using an offline version of the CAM 3.0 radiation calculations that we modified to run as a single column. The mean state of all variables in the offline radiation model are set to the mean of the C-IO control run, and the aerosols are prohibited from taking up water. For each experiment either surface albedo or specific humidity are modified while all other variables are held fixed.

Water vapor is partitioned into pools based on the relative contribution of each source term over the entire area north of 60 °N compared to the only sink (precipitation). At steady state, the sum of all sources (ET, ocean evaporation (OE), and import) is equal to precipitation (P), therefore we can show the relative contribution of each term as the ratio between the source and P. The estimate of water vapor q from one source (in this case ET) is calculated as:

$$q^{\mathrm{ET}} = \left(\frac{\mathrm{ET}}{P}\right) \cdot q^{\mathrm{total}},$$

where q^{total} is the specific humidity (mass of water vapor), ET is evapotranspiration and P is precipitation. The sensitivity of the radiative forcing in the 1D offline radiation model to each input of water vapor is then estimated by comparing the forcing in both short-wave and long-wave from q and $q + \Delta q$ where Δq is calculated as

$$\Delta q^{\mathrm{ET}} = \left(\frac{\mathrm{ET}}{P}\right)_{\mathrm{EXP}} \cdot q^{\mathrm{total}}_{\mathrm{EXP}} - \left(\frac{\mathrm{ET}}{P}\right)_{\mathrm{CON}} \cdot q^{\mathrm{total}}_{\mathrm{CON}}$$

and *EXP* and *CON* denote values from the experiment and control calculations respectively. Offline radiation calculations were performed for the average monthly radiation conditions at eight daily time steps and results shown are averaged over all times steps for the specified months. ΔF is calculated as the difference in the radiative fluxes from a run with albedo or specific humidity equal to the mean of V-FO and a run with albedo or specific humidity equal to the mean of C-FO while all other variables in the radiation calculation are held fixed as C-IO. ΔF is reported as an average over the entire Arctic region (north of 60 °N) for changes in water vapor and as an average over either Arctic Land or Ocean area for changes in albedo.

ACKNOWLEDGMENTS. W. Collins provided the radiation model and C. Bitz, W. Collins, D. Feldman, and M. Vizciano provided assistance with model configuration, M. Jones provided discussion on the nature of Arctic vegetation and its paleo-extent and P.J. Sellers had many helpful suggestions in his review. A. Stine, M. Vizciano, and J. E. Lee provided comments on this manuscript. We acknowledge National Science Foundation Award ATM-0628678 to the University of California, Berkeley and National Science Foundation Award ATM-0628582 to the Woods Hole Oceanographic Institution. The National Center for Atmospheric Research is sponsored by the National Science Foundation.

1. Lloyd A (2005) Ecological histories from Alaskan tree lines provide insight into future change. *Ecology*, 86:1687–1695.
2. Bonan GB (2008) Forests and climate change: Forcings, feedbacks, and the climate benefits of forests. *Science*, 320:1444–1449.
3. Fischlin A, et al. (2007) *Climate Change 2007: Impacts, Adaptation and Vulnerability. Contributionof Working Group II to the Fourth Assessment Report of the Intergovernmental Panel on Climate Change*, eds Parry ML, et al. (Cambridge Univ. Press, Cambridge UK and New York), pp 211–272.
4. Edwards M, Brubaker L, Lozhkin A, Anderson P (2005) Structurally novel biomes: A response to past warming in Beringia. *Ecology*, 86:1696–1703.
5. Liu H, Randerson J, Lindfors J, Chapin F (2005) Changes in the surface energy budget after fire in boreal ecosystems of interior Alaska: An annual perspective. *J Geophys Res*, 110:D13101.
6. Bonan GB, Pollard D, Thompson SL (1992) Effects of boreal forest vegetation on global climate. *Nature*, 359:716–718.
7. Foley JA, Kutzbach J, Coe MT, Levis S (1994) Feedbacks between climate and boreal forests during the holocene epoch. *Nature*, 371:52–54.
8. Levis S, Foley J, Pollard D (1999) Potential high-latitude vegetation feedbacks on CO_2-induced climate change. *Geophys Res Lett*, 26:747–750.
9. Snyder P, Delire C, Foley J (2004) Evaluating the influence of different vegetation biomes on the global climate. *Clim Dynam*, 23:279–302.
10. Cook BI, Bonan GB, Levis S, Epstein HE (2008) Rapid vegetation responses and feedbacks amplify climate model response to snow cover changes. *Clim Dynam*, 30:391–406.
11. Chapin F, et al. (2000) Arctic and boreal ecosystems of western North America as components of the climate system. *Glob Change Biol*, 6:211–223.
12. Eugster W, et al. (2000) Land-atmosphere energy exchange in Arctic tundra and boreal forest: Available data and feedbacks to climate. *Glob Change Biol*, 6:84–115.
13. McGuire AD, Chapin FSI, Walsh JE, Wirth C (2006) Integrated regional changes in Arctic climate feedbacks: Implications for the global climate system. *Annu Rev Env Resour*, 31:61–91.
14. Rupp T, Chapin F, Starfield A (2000) Response of subarctic vegetation to transient climatic change on the seward peninsula in north-west alaska. *Glob Change Biol*, 6:541–555.
15. Peros MC, Gajewski K, Viau AE (2008) Continental-scale tree population response to rapid climate change, competition, and disturbance. *Global Ecol Biogeogr*, 17:658–669.
16. Chapin F, Starfield A (2007) Time lags and novel ecosystems in response to transient climatic change in arctic alaska. *Climatic Change*, 35:449–461.
17. Danby RK, Hik DS (2007) Variability, contingency, and rapid change in recent subarctic alpine tree line dynamics. *J Ecol*, 95:352–363.
18. Christensen J, et al. (2007) *Climate Change 2007: The Scientific Basis, Contribution of Working Group I to the Fourth Assessment Report of the Intergovernmental Panel on*

Climate Change, eds Solomon S, et al. (Cambridge Univ. Press, Cambridge UK and New York), pp 847–940.
19. Hansen J, et al. (2005) Efficacy of climate forcings. *J Geophys Res*, 110:D18104.
20. Collins W, et al. (2006) The formulation and atmospheric simulation of the community atmosphere model version 3 (CAM3). *J Climate*, 19:2144–2161.
21. Doney SC, Lindsay K, Fung I, John J (2006) Natural variability in a stable, 1000-yr global coupled climate-carbon cycle simulation. *J Climate*, 19:3033–3054.
22. Kiehl J, Shields C, Hack J, Collins W (2006) The climate sensitivity of the community climate system model version 3 (CCSM3). *J Climate*, 19:2584–2596.
23. Oleson KW, et al. (2008) Improvements to the community land model and their impact on the hydrological cycle. *J Geophys Res*, 113:G01021.
24. Rasch PJ, Williamson DL (1990) On shape-preserving interpolation and semi-lagrangian transport. *SIAM J. Sci. Stat. Comput*, 11:656–687.